



Published in final edited form as:

Cancer Res. 2009 July 15; 69(14): 5829–5834. doi:10.1158/0008-5472.CAN-08-3465.

Pre-clinical development of a bi-functional cancer cell homing, PKC ϵ inhibitory peptide for the treatment of head and neck cancer

Liwei Bao¹, Michael A. Gorin², Manchao Zhang³, Alejandra C. Ventura¹, William C. Pomerantz⁴, Sofia D. Merajver¹, Theodoros N. Teknos^{3,5}, Anna K. Mapp⁴, and Quintin Pan^{3,5}

¹ Department of Internal Medicine, Division of Hematology and Oncology, University of Michigan, Medical School, Ann Arbor, MI 48109

² Miller School of Medicine, University of Miami, Miami, FL 33136

³ Arthur G. James Cancer Hospital and Richard J. Solove Research Institute, The Ohio State University, Comprehensive Cancer Center, Columbus, OH 43210

⁴ Department of Chemistry, University of Michigan, Ann Arbor, MI 48109

⁵ Department of Otolaryngology-Head and Neck Surgery, The Ohio State University Medical Center, Columbus, OH 43210

Abstract

Head and neck squamous cell carcinoma (HNSCC) is the sixth most frequent cancer worldwide, comprising almost 50% of all malignancies in some developing nations. Our recent work identified protein kinase C ϵ (PKC ϵ) as a critical and causative player in establishing an aggressive phenotype in HNSCC. In this study, we investigated the specificity and efficacy of HN1-PKC ϵ , a novel bi-functional cancer cell homing, PKC ϵ inhibitory peptide, as a treatment for HNSCC. HN1-PKC ϵ peptide was designed by merging two separate technologies and synthesized as a capped peptide with two functional modules, HN1 (cancer cell homing) and PKC ϵ (specific PKC ϵ inhibitory), connected by a novel linker module. HN1-PKC ϵ preferentially internalized into UMSCC1 and UMSCC36 cells, two HNSCC cell lines, in comparison to oral epithelial cells; 82.1% positive for UMSCC1 and 86.5% positive for UMSCC36 compared to 1.2% positive for oral epithelial cells. In addition, HN1-PKC ϵ penetrated HNSCC cells in a dose- and time-dependent manner. Consistent with these *in vitro* observations, systemic injection of HN1-PKC ϵ resulted in selective delivery of HN1-PKC ϵ into UMSCC1 xenografts in nude mice. HN1-PKC ϵ blocked the translocation of active PKC ϵ in UMSCC1 cells confirming HN1-PKC ϵ as a PKC ϵ inhibitor. HN1-PKC ϵ inhibited cell invasion by $72 \pm 2\%$ ($p < 0.001$, $n = 12$) and cell motility by $56 \pm 2\%$ ($p < 0.001$, $n = 5$) in UMSCC1 cells. Moreover, *in vivo* bioluminescence imaging demonstrated that HN1-PKC ϵ significantly ($83 \pm 1\%$ inhibition, $p < 0.02$) retards the growth of UMSCC1 xenografts in nude mice. Our work indicates that the bi-functional HN1-PKC ϵ inhibitory peptide represents a promising novel therapeutic strategy for HNSCC.

Keywords

Experimental therapeutics; Head and Neck Cancer; Protein Kinase; and Oncogene

INTRODUCTION

Head and neck squamous cell carcinoma (HNSCC) is the sixth most frequent cancer worldwide. Nearly 46,000 people will be diagnosed with HNSCC in the United States this year and an estimated 11,000 people will die of the disease (1). Although improvements in local control and survival have been achieved with the use of multi-modality regimens, the overall 5 year survival rate for HNSCC has not improved significantly over the past 20 years (2,3). Local-regional relapse and distant metastasis after definitive therapy remain the major causes of morbidity and mortality in HNSCC patients. This clinical problem has prompted substantial efforts in identifying genetic determinants that contribute to aggressive HNSCC.

Evidence has shown that protein kinase C ϵ (PKC ϵ), a member of a family of serine/threonine protein kinases, is a transforming oncogene and is involved in the development and progression of skin, breast, and prostate cancer (4–6). Our recent results demonstrate that PKC ϵ plays a critical and causative role in establishing an aggressive phenotype in HNSCC. We reported that PKC ϵ is upstream of and directly modulates the Rho GTPase signaling cascade, specifically RhoA and RhoC, to control cell invasion and motility (7). Moreover, specific inhibition of PKC ϵ with RNA interference in HNSCC cells with high endogenous PKC ϵ levels was sufficient to significantly inhibit cell invasion and motility (7). A prospective study showed that elevated PKC ϵ in the primary tumor of HNSCC patients is associated with an increase in disease recurrence and a decrease in overall survival (8). This observation is in agreement with our work that PKC ϵ promotes an aggressive phenotype in HNSCC and suggests that targeting PKC ϵ may be an effective anti-cancer strategy for managing HNSCC patients.

In this study, we determined the effects of a novel cancer cell homing, PKC ϵ inhibitory peptide on HNSCC cells *in vitro* and *in vivo*. The bi-functional HN1-PKC ϵ peptide was constructed by connecting two functional motifs, HN1 (cancer cell homing) and PKC ϵ (specific PKC ϵ inhibitory), with a linker peptide. HN1-PKC ϵ preferentially penetrated HNSCC cells *in vitro* and *in vivo* and blocked the translocation of active PKC ϵ in HNSCC cells. In addition, HN1-PKC ϵ inhibited cell invasion, motility, and proliferation *in vitro* and significantly retarded the growth of HNSCC xenografts in nude mice. Our work shows that HN1-PKC ϵ is a novel therapeutic agent with potent anti-tumor efficacy against HNSCC.

MATERIALS AND METHODS

Cell lines

Immortalized normal oral epithelial cells (E6/E7-NOE) were kindly provided by Drs. William Foulkes and Ala-Eddin Al Moustafa from McGill University and cultured in Keratinocyte-SFM medium without supplement. UMSCC1 and UMSCC36 cells were kindly provided by Dr. Thomas Carey from the University of Michigan Medical School and cultured in DMEM supplemented with 10% fetal bovine serum.

Peptide synthesis

Unlabeled and FITC-labeled peptides were synthesized and purified (>95%) by the University of Michigan Protein Structure and Peptide Synthesis Facility or by New England Peptides (Gardner, MA). Cy5-labeled HN1-PKC ϵ was synthesized and purified (>95%) by Open Biosystems (Huntsville, AL). Cy5-labeled PKC ϵ was synthesized by standard N-9-fluorenylmethoxycarbonyl (Fmoc) solid phase synthesis on CLEAR amide resin (Peptide International, 0.48 mmol/g). Following Fmoc deprotection of the final residue, 2 equivalents of Cy5-NHS ester (GE Healthcare, United Kingdom) and 4 equivalents of triethylamine were dissolved in NMP and transferred to the resin. The reaction vessel was covered in foil and left to react for 16 hrs. The resin was washed 3 \times DMF, 3 \times CH₂Cl₂ and 3 \times MeOH. The Cy5-

labeled PKC ϵ peptide was cleaved from the resin for two hours in a mixture of 95/2.5/2.5 trifluoroacetic acid (TFA)/triisopropylsilane/water. The crude peptide was precipitated into cold ether and purified by RP-HPLC on a Waters C18 column using water with 0.1% TFA as the A solvent and CH₃CN as the B solvent (14%–31%B over 17 minutes). Product molecular weight was confirmed by ESI-MS in both negative ion mode ($m-H^+$, 1479.1) and positive ion mode ($M+2H^+/2$, 740.9).

PKC ϵ translocation

UMSCC1 cells were untreated or treated with HN1-control or HN1-PKC ϵ for 48 hours. Subsequently, cells were stimulated with a general PKC activator, phorbol 12-myristate 13-acetate (PMA, 10 nM for 30 minutes), washed with cold phosphate-buffered saline, scraped in homogenization buffer (9), passed through a 25-gauge syringe needle, and spun at $100,000 \times g$ for 30 minutes at 4°C. The cytoplasmic fractions were collected and the pellets (particulate fractions) were resuspended in homogenization buffer with 1% Triton X-100. Western blot analysis using a PKC ϵ -specific antibody (Millipore, Billerica, MA) was performed to assess the translocation of PKC ϵ .

Cell invasion and cell motility

Cell invasion was determined as described from the cell invasion assay kit (Chemicon International, Temecula, CA). Cells were harvested and resuspended in serum-free medium. An aliquot (1×10^5 cells) of the prepared cell suspension was added into the chamber and incubated for 24 hours at 37°C in a 10% CO₂ tissue culture incubator. Non-invading cells were gently removed from the interior of the inserts with a cotton-tipped swab. Invasive cells were stained and counted. Random cell motility was determined as described from the motility assay kit (Cellomics, Pittsburgh, PA). Cells were harvested, suspended in medium and plated on top of a field of microscopic fluorescent beads. After a 16-hour incubation period, cells were fixed and areas of clearing in the fluorescent bead field corresponding to phagokinetic cell tracks were quantified using NIH ScionImager.

Cell proliferation

Cells were untreated or treated with cis-platinum (1, 3, or 10 μ M), cis-platinum and HN1-control, or cis-platinum and HN1-PKC ϵ for 3 days. Cell proliferation was assessed using the MTT reagent to detect metabolic active cells (Sigma, St. Louis, MO).

Pre-clinical efficacy of HN1-PKC ϵ

UMSCC1-luciferase cells (1×10^6) were implanted into the flank of 10-week old athymic nude mice and tumors were allowed to develop without treatment. At 2-weeks post-implantation, mice with established tumors of approximately 40 mm³ in volume were imaged for bioluminescence intensity using the Xenogen IVIS Spectrum System (Caliper Life Sciences, Hopkinton, MA). Mice were randomly assigned to three treatment arms, untreated (n=9), HN1-control (10 mg/kg, 3X week, n=8) or HN1-PKC ϵ (10 mg/kg, 3X week, n=11), based on bioluminescence intensity to achieve a statistically similar mean bioluminescence intensity at the start of the treatment protocol. Tumor response was assessed on a weekly basis using the *in vivo* bioluminescence imaging modality.

Statistical analysis

Data were analyzed by Student's *t*-test. P-values<0.05 were considered significant

RESULTS AND DISCUSSION

The excitement over PKCs as therapeutic anti-cancer targets prompted the rapid development of drugs designed to specifically inhibit PKCs. The drugs developed to date can be divided into two main groups; inhibitors that target the C1 regulatory domain and inhibitors that target the kinase domain. Overall, in numerous clinical trials, PKC inhibitors have shown very modest activity, at best, as single agent or in combination with standard chemotherapeutics (10,11). Bryostatin-1, a PKC modulator that targets the C1 domain, is the most extensively used in clinical trials. Recent phase II clinical trials with bryostatin-1 in combination with cisplatin for cervical squamous cell carcinoma or in combination with interleukin-2 for renal cell carcinoma showed minimal efficacy and perhaps even a possibility of therapeutic antagonism (12,13). One possible explanation is that C1 domain inhibitors are not isoform specific since the C1 domain is well conserved in the PKC family, with the exception of the atypical isoforms. Therefore, C1 domain inhibitors likely inhibit desired oncogene-like PKC isoforms but also have the undesired side-effect of inhibiting tumor-suppressor-like PKC isoforms resulting in no net response or possibly a tumor stimulatory response. The kinase domain inhibitors are not specific PKC inhibitors since the kinase inhibitors target other serine/threonine kinases with higher specificity. Taken together, there remains a critical need to develop isoform specific PKC inhibitors.

The activation of the PKC ϵ signaling cascade is a critical genetic event resulting in an aggressive HNSCC phenotype. Our laboratory reported that RhoA and RhoC are directly phosphorylated by PKC ϵ resulting in an increase in RhoA/RhoC activation (7). In addition to regulation of RhoA and RhoC, other groups have published that PKC ϵ directly phosphorylates Akt and Stat3. PKC ϵ phosphorylates Akt at serine 473 leading to a full Akt activation state (14). A recent report showed that PKC ϵ phosphorylates Stat3 at Ser727 resulting in an increase in nuclear translocation and transcriptional activation of Stat3 (15). Elevated Akt phosphorylation (Ser473) significantly correlates with a worse outcome in HNSCC (16,17). Nuclear Stat3 accumulation is associated with a decrease in relapse-free and overall survival in HNSCC (18). Thus, targeting PKC ϵ is an attractive therapeutic strategy as inhibition of PKC ϵ will result in dampening of multiple signal transduction pathways that are dysregulated in HNSCC.

Protein-protein interactions are critical events in numerous signaling pathways. However, since protein to protein interfaces are usually extensive, shallow, and hydrophobic, the disruption of protein-protein interactions has proven to be difficult targets for small-molecule drugs. So, we decided to take a different approach and rationally designed a bi-functional targeting peptide. We merged two existing and published technologies and constructed a peptide with two functional modules, HN1 and PKC ϵ , connected by a linker module. The HN1 module is a 12-mer peptide, TSPLNIHNGQKL, reported to preferentially bind and internalize into HNSCC cell lines *in vitro* (19). Moreover, HN1 was demonstrated to be stable *in vivo* and able to localize into HNSCC xenograft tumors (19). The PKC ϵ inhibitory module (ϵ V1-2) is an 8-mer peptide, EAVSLKPT, taken from amino acids 14–21 located in the pseudo-C2 domain of PKC ϵ (20). There is literature to demonstrate that the pseudo-C2 domain of PKC ϵ is required for binding to receptors of activated protein kinase C (RACKs) (21,22). The PKC ϵ -RACK interaction allows for the proper trafficking and localization of active PKC ϵ (21,22). The RACK binding site on PKC ϵ was reported to be a discrete region located at amino acids 14–21 (20). A peptide (ϵ V1-2) corresponding to this sequence inhibited the translocation and function of active PKC ϵ through blocking the PKC ϵ -RACK interaction in cardiac myocytes (20). Moreover, ϵ V1-2 was shown to be a specific PKC ϵ inhibitor and not able to block the translocation and function of other PKCs, specifically PKC α , β and δ (20). Subsequent work has clearly demonstrated that ϵ V1-2 is a specific PKC ϵ inhibitor in other cell types, including neuronal cells and pancreatic β -cells (23,24). The control module is a non-functional scrambled PKC ϵ

peptide, LSETKPAV (20). The linker module consists of a 6-mer sequence of 6-aminohexanoic acid to allow for proper spatial spacing to prevent steric interference between the HN1- and PKC ϵ -targeting modules.

To determine the efficiency and selectivity of HN1-PKC ϵ for HNSCC cells *in vitro*, oral epithelial cells (NOE), UMSSC1, and UMSSC36 were untreated or treated with a series of different fluorescein isothiocyanate (FITC)-labeled peptides (3 μ M for 48 hours), followed by fluorescence-activated cell sorting (FACS) analysis (Figure 1A). NOE cells treated with FITC-labeled HN1-PKC ϵ had minimal effect and resulted in 1.2% FITC-positive cells with a mean fluorescence intensity of 1.9. In contrast, FITC-labeled HN1-PKC ϵ treatment of UMSSC1 and UMSSC36 cells resulted in 82.1% and 86.5% FITC-positive cells, respectively. The mean fluorescence intensity was 15.9 for UMSSC1 cells and 18.3 for UMSSC36 cells with FITC-labeled HN1-PKC ϵ treatment. As expected, treatment with FITC-labeled scramble-PKC ϵ , a peptide with an inactive cancer cell homing module, was not as efficient and resulted in 10.2% FITC-positive cells for UMSSC1 and 5.3% FITC-positive cells for UMSSC36. It is clear that FITC-labeled HN1-PKC ϵ is greater than 8-fold more efficient ($p < 0.03$) than FITC-labeled scramble-PKC ϵ providing evidence that the addition of the functional HN1 cancer cell homing module is a critical value-added feature to enhance the uptake of the PKC ϵ inhibitory module in HNSCC cells. Treatment with FITC-labeled HN1-control had a similar effect as FITC-labeled HN1-PKC ϵ and resulted in 82.6% FITC-positive cells for UMSSC1 and 82.7% FITC-positive cells for UMSSC36. This is an important observation and demonstrates that modification of the amino acid sequence order of the PKC ϵ inhibitory module to a nonfunctional scrambled control version does not alter the internalization efficiency into HNSCC cells. Interestingly, FITC-labeled PKC ϵ is more efficient than FITC-labeled scramble-PKC ϵ . A likely explanation is that the uptake of FITC-labeled peptides into HNSCC cells is mass/size-dependent since FITC-labeled scramble-PKC ϵ consists of 26 amino acid residues and FITC-labeled PKC ϵ consists of only 8 amino acid residues. Nonetheless, the internalization efficiency of FITC-labeled HN1-PKC ϵ is superior to FITC-labeled PKC ϵ ($p < 0.04$). Lastly, as shown in Figures 1C and D, a dose- and time-dependent uptake of FITC-labeled HN1-PKC ϵ was observed in UMSSC1 and UMSSC36 cells.

Next, we examined if HN1-PKC ϵ specifically localizes to HNSCC tumors *in vivo*. We decided to use Cy5 as the fluorophore for this experiment since Cy5 exhibits longer excitation and emissions wavelengths than FITC and thus, enables deeper tissue penetration. Athymic nude mice with established UMSSC1 tumors in the flank were untreated or treated with Cy5-labeled PKC ϵ or HN1-PKC ϵ (10 mg/kg by intraperitoneal injection). After 24 hours, mice were euthanized and tumors and various organs were resected for fluorescence intensity analysis using the Xenogen IVIS Spectrum Imaging System (Figure 2). *Ex vivo* analysis showed that the tumors and various organs resected from untreated or Cy5-labeled PKC ϵ -treated mice exhibit minimal fluorescence. In contrast, Cy5-labeled HN1-PKC ϵ was selectively delivered to the HNSCC tumor. Fluorescence intensity was greater than 8-fold higher ($p < 0.0001$) in the tumor compared to the various organs in Cy5-labeled HN1-PKC ϵ -treated mice. These results showed that HN1-PKC ϵ selectively homed to and penetrated into HNSCC tumors *in vivo*.

Our work corroborated the findings from Hong and Clayman (19) and demonstrated that the HN1 motif selectively homes and penetrates HNSCC cells in comparison to immortalized oral epithelial cells. Furthermore, we have evidence that HN1-PKC ϵ does not internalize into primary keratinocytes (data not shown). Hong and Clayman reported that HN1 did not internalize into DU145 human prostate cancer cells, SW480 human colon cells, and U373 MG human astrocytoma cells suggesting that HN1 may be specific to squamous cell carcinoma (19). However, this is not the case as HN1-PKC ϵ efficiently internalized into MDA-MB231 (70.1% FITC-positive; mean fluorescence intensity of 64.2) and SKBR3 (49.4% FITC-positive; mean fluorescence intensity of 27.3) human breast cancer cells. Interestingly, HN1-

PKC ϵ penetrated MCF10A nontumorigenic mammary epithelial cells with much lower efficiency (8.8% FITC-positive; mean fluorescence intensity of 5.9). These results provide initial evidence that HN1 may be cancer cell-specific but not organ-specific. Our observations do not detract from the significance and utility of HN1 but rather expands the potential clinical use of HN1 to other cancer types.

The PKC ϵ inhibitory module was demonstrated to selectively block the translocation of active PKC ϵ in numerous cell types, including cardiac myocytes, pancreatic β -cells, and neuronal cells (19,23,24). There is evidence to indicate that inactive PKC ϵ is localized in the cytoplasmic fraction and upon activation translocates to the particulate fraction (25,26). To determine if HN1-PKC ϵ can block the translocation of active PKC ϵ in HNSCC cells, UMSSC1 cells were untreated or incubated with HN1-control or HN1-PKC ϵ for 24 hours. Subsequently, cells were activated with PMA and cell lysates were fractionated for cytoplasmic and particulate proteins. As shown in Figure 3A, active PKC ϵ is dramatically lower in HN1-PKC ϵ -treated cells than in untreated or HN1-control treated cells. These results provide direct evidence that HN1-PKC ϵ disrupts the proper localization of PKC ϵ resulting in “normalization” of active PKC ϵ levels in HNSCC cells.

We determined the effects of HN1-PKC ϵ on cell invasion, cell motility, and cell proliferation. UMSSC1 cells were untreated or incubated with 30 μ M HN1-control and HN1-PKC ϵ for 72 hours. Subsequently, cells were trypsinized and re-plated in appropriate experimental wells to assess for cell invasion and cell motility. UMSSC1 cells treated with HN1-PKC ϵ were significantly less invasive and motile than untreated cells or HN1-control treated cells (Figures 3B and 3C). HN1-PKC ϵ inhibited cell invasion by $72 \pm 2\%$ ($p < 0.001$, $n=12$) and cell motility was suppressed by $56 \pm 2\%$ ($p < 0.001$, $n=5$) in UMSSC1 cells. As shown in Figure 3D, the effects of HN1-PKC ϵ on cell proliferation as monotherapy or in combination therapy with cis-platinum was assessed. As expected, cis-platinum (no peptide treatment) inhibited cell proliferation in a dose-dependent manner; ranging from $3 \pm 1\%$ inhibition for 1 μ M to $49 \pm 2\%$ inhibition for 10 μ M. HN1-control (30 μ M for 72 hours) had no effect on cell proliferation as monotherapy and no additional effect was observed in combination with cis-platinum. Single agent treatment of HN1-PKC ϵ (30 μ M for 72 hours) significantly inhibited cell proliferation by $39 \pm 2\%$ and moreover, used in a combination treatment regimen, an additive effect is observed with cis-platinum. Single agent cis-platinum (10 μ M for 72 hours) inhibited cell proliferation by $49 \pm 2\%$, whereas, the combination regimen of 30 μ M HN1-PKC ϵ and 10 μ M cis-platinum for 72 hours inhibited cell proliferation by $72 \pm 4\%$. The combination regimen resulted in a 47% increase in inhibition of cell proliferation compared to single agent cis-platinum treatment. This observation supports the notion that the combination regimen of a PKC ϵ inhibitor and cis-platinum is more efficacious than either single agent therapy alone. It is critical to point out that the HN1 module does not have anti-cancer properties as the HN1-control peptide had no effect on cell invasion, motility, and proliferation. These observations strongly indicate that the PKC ϵ inhibitory module is solely responsible for the anti-tumor effects as observed in these phenotypic experiments.

The anti-tumor efficacy of HN1-PKC ϵ was assessed in a xenograft model of HNSCC. UMSSC1 cells were infected with a lentivirus expression vector to drive constitutive *Firefly* luciferase (pLentiox-Luc) to allow us to measure tumor response using a highly sensitive and dynamic *in vivo* bioluminescence imaging modality. UMSSC1-luciferase cells (1×10^6) were implanted into the flank of 10-week old athymic nude mice and tumors were allowed to develop without treatment. At 2-weeks post-implantation, mice with established tumors of approximately 40 mm³ in volume were imaged for bioluminescence intensity. Mice were randomly assigned to three treatment groups, untreated ($n=9$), HN1-control (10 mg/kg intraperitoneal injection, 3X week, $n=8$), or HN1-PKC ϵ (10 mg/kg intraperitoneal injection, 3X week, $n=11$) based on bioluminescence intensity to achieve a statistically similar mean

bioluminescence intensity at the start of the treatment protocol. At the end of the 4 week treatment protocol, mean tumor bioluminescence intensity between the untreated arm and HN1-control-treated arm was statistically similar ($p>0.05$); 15.2 ± 5.2 photons/s for the untreated mice and 11.0 ± 3.9 photons/s for the HN1-control-treated mice (Figure 4B). Mice from the HN1-PKC ϵ treatment arm showed a dramatic difference and had a mean tumor bioluminescence intensity of only 1.9 ± 0.9 photons/s. Mean tumor bioluminescence intensity was about 5.8-fold higher in the HN1-control arm in comparison to the HN1-PKC ϵ arm ($p<0.02$). As shown in Figure 4C, immunohistochemistry staining indicated that HN1-PKC ϵ treatment resulted in a $71 \pm 8\%$ decrease in the tumor proliferation index and a $314 \pm 29\%$ increase in the tumor apoptotic index compared to HN1-control treatment ($p<0.001$). Additionally, pStat3 (S727) levels, a downstream target of active PKC ϵ , were markedly lower in the tumors from the HN1-PKC ϵ arm than from the untreated or HN1-control arm. These *in vivo* results demonstrate a robust anti-tumor effect with HN1-PKC ϵ treatment in HNSCC.

The paradigm of molecularly-targeted anti-cancer therapies is beginning to take hold. To date, several molecularly-targeted anti-cancer therapies, such as bevacizumab and cetuximab, have proven to be effective approaches for managing cancer patients. Many of these molecularly-targeted anti-cancer agents have shown to be more selective for cancer cells and thus exhibit lower overall toxicity profiles than standard chemotherapeutics. Nevertheless, dose-limiting toxicities, most likely due to drug delivery to non-target cells and organs, remain a critical issue even with molecularly-targeted anti-cancer drugs. Development of a bi-functional anti-cancer drug consisting of a molecularly-targeted therapeutic and a tumor-targeting component will enable the specific delivery of an anti-cancer therapeutic to tumor cells resulting in increased local efficacy while limiting peripheral toxicity. HN1-PKC ϵ was conceived with these two criteria in mind. Our results clearly demonstrate that HN1-PKC ϵ is functioning as designed and selectively penetrates HNSCC cells to inhibit active PKC ϵ translocation. Systemic administration of HN1-PKC ϵ significantly retarded the growth of HNSCC xenograft as measured by a highly sensitive *in vivo* bioluminescence imaging modality. There was no apparent difference in the weight of untreated, HN1-control-treated, and HN1-PKC ϵ -treated mice during the active treatment period providing initial evidence that HN1-PKC ϵ has a favorable toxicity profile. Taken together, this study indicates that HN1-PKC ϵ has potent anti-tumor effects and further development of HN1-PKC ϵ as an anti-cancer therapeutic for HNSCC is warranted.

Acknowledgments

Work supported in part by from the National Cancer Institute, P50CA97248 and R01CA135096, and the Flight Attendant Medical Research Institute.

References

1. Jemal A, Siegel R, Ward E, Murray T, Xu J, Thun MJ. Cancer Statistics, 2007. *CA Cancer J Clin* 2007;57:43–66. [PubMed: 17237035]
2. Funk GF, Karnell LH, Robinson RA, Zhen WK, Trask DK, Hoffman HT. Presentation, treatment, and outcome of oral cavity cancer: a National Cancer Data Base report. *Head Neck* 2002;24:165–80. [PubMed: 11891947]
3. Pugliano FA, Piccirillo JF, Zequeria MR, Fredrickson JM, Perez CA, Simpson JR. Clinical severity staging system for oral cavity cancer: five year survival. *Otolaryngol Head Neck Surg* 1999;120:38–45. [PubMed: 9914547]
4. Jansen AP, Verwiebe EG, Dreckschmidt NE, Wheeler DL, Oberley TD, Verma AK. Protein kinase C-epsilon transgenic mice: a unique model for metastatic squamous cell carcinoma. *Cancer Res* 2001;61:808–12. [PubMed: 11221859]

5. Pan Q, Bao LW, Kleer CG, et al. Protein kinase C ϵ is a predictive biomarker of aggressive breast cancer and a validated target for RNA interference anti-cancer therapy. *Cancer Res* 2005;65:8366–71. [PubMed: 16166314]
6. Wu D, Foreman TL, Gregory CW, et al. Protein kinase Cepsilon has the potential to advance the recurrence of human prostate cancer. *Cancer Res* 2002;62:2423–9. [PubMed: 11956106]
7. Pan Q, Bao LW, Teknos TN, Merajver SD. Targeted disruption of PKC ϵ reduces cell invasion and motility through inactivation of RhoA and RhoC GTPases in head and neck squamous cell carcinoma. *Cancer Res* 2006;66:9379–84. [PubMed: 17018591]
8. Martinez-Gimeno C, Diaz-Meco MT, Dominguez I, Moscat J. Alterations in levels of different protein kinase C isotypes and their influence on behavior of squamous cell carcinoma of the oral cavity: epsilonPKC, a novel prognostic factor for relapse and survival. *Head Neck* 1995;17:516–25. [PubMed: 8847210]
9. Schechtman D, Mochly-Rosen D. Isozyme-specific inhibitors and activators of protein kinase C. *Methods Enzymol* 2002;345:470–89. [PubMed: 11665630]
10. Mackay HJ, Twelves CJ. Protein kinase C: a target for anticancer drugs? *Endocr Relat Cancer* 2003;10:389–96. [PubMed: 14503915]
11. Serova M, Ghouli A, Benhadji KA, et al. Preclinical and clinical development of novel agents that target the protein kinase C family. *Semin Oncol* 2006;33:466–78. [PubMed: 16890801]
12. Nezhat F, Wadler S, Muggia F, et al. Phase II trial of the combination of bryostatin-1 and cisplatin in advance or recurrent squamous cell carcinoma of the cervix: a New York Gynecologic Oncology Group study. *Gynecol Oncol* 2004;93:144–8. [PubMed: 15047228]
13. Peterson AC, Harlin H, Karrison T, et al. A randomized phase II trial of interleukin-2 in combination with four different doses of bryostatin-1 in patients with renal cell carcinoma. *Invest New Drugs* 2006;24:141–9. [PubMed: 16514482]
14. Zhang J, Baines CP, Zong C, et al. Functional proteomic analysis of a three-tier PKC-epsilon-Akt-eNOS signaling module in cardiac protection. *Am J Physiol Heart Circ Physiol* 2004;288:H954–61. [PubMed: 15528226]
15. Aziz MH, Manoharan HT, Verma AK. Protein kinase C ϵ , which sensitizes skin to sun's UV radiation-induced cutaneous damage and development of squamous cell carcinomas, associates with Stat3. *Cancer Res* 2007;63:1385–93. [PubMed: 17283176]
16. Lim J, Kim JH, Paeng JY, et al. Prognostic value of activated Akt expression in oral squamous cell carcinoma. *J Clin Pathol* 2005;58:1199–205. [PubMed: 16254112]
17. Massarelli E, Liu DD, Lee JJ, et al. Akt activation correlates with adverse outcome in tongue cancer. *Cancer* 2005;104:2430–6. [PubMed: 16245318]
18. Shah NG, Trivedi TI, Tankshali RA, et al. Stat3 expression in oral squamous cell carcinoma: association with clinical parameters and survival. *Int J Biol Markers* 2006;21:175–83. [PubMed: 17013800]
19. Hong FD, Clayman GL. Isolation of a peptide for targeted drug delivery into human head and neck solid tumors. *Cancer Res* 2000;60:6551–6. [PubMed: 11118031]
20. Johnson JA, Gray MO, Chen C, Mochly-Rosen D. A protein kinase C translocation inhibitor as a isozyme-selective antagonist of cardiac function. *J Biol Chem* 1996;271:24962–6. [PubMed: 8798776]
21. Csukai M, Chen CH, De Matteis MA, Mochly-Rosen D. The coatamer protein β' -COP, a selective binding protein (RACK) for protein kinase C ϵ . *J Biol Chem* 1997;272:29200–06. [PubMed: 9360998]
22. Besson A, Wilson TL, Yong VW. The anchoring protein RACK1 links protein kinase Cepsilon to integrin beta chains. Requirements for adhesion and motility. *J Biol Chem* 2002;277:22073–84. [PubMed: 11934885]
23. Yedovitzky M, Mochly-Rosen D, Johnson JA, et al. Translocation inhibitors define specificity of protein kinase C isoenzyme in pancreatic b-cells. *J Biol Chem* 1997;272:1417–20. [PubMed: 8999804]
24. Hundle B, McMahon T, Dadgar J, Chen CH, Mochly-Rosen D, Messing RO. An inhibitory fragment derived from protein kinase Cepsilon prevents enhancement of nerve growth factor responses by ethanol and porbol esters. *J Biol Chem* 1997;272:15028–35. [PubMed: 9169479]

25. Xiao GQ, Qu Y, Sun ZQ, Mochly-Rosen D, Boutjdir M. Evidence for functional role of epsilonPKC isozyme in the regulation of cardiac Na(+) channels. *Am J Physiol Cell Physiol* 2001;281:C1477–86. [PubMed: 11600410]
26. Brandman R, Disatnik MH, Churchill E, Mochly-Rosen D. Peptides derived from the C2 domain of protein kinase C epsilon (epsilon PKC) modulate epsilon PKC activity and identify potential protein-protein interaction surfaces. *J Biol Chem* 2007;282:4113–23. [PubMed: 17142835]

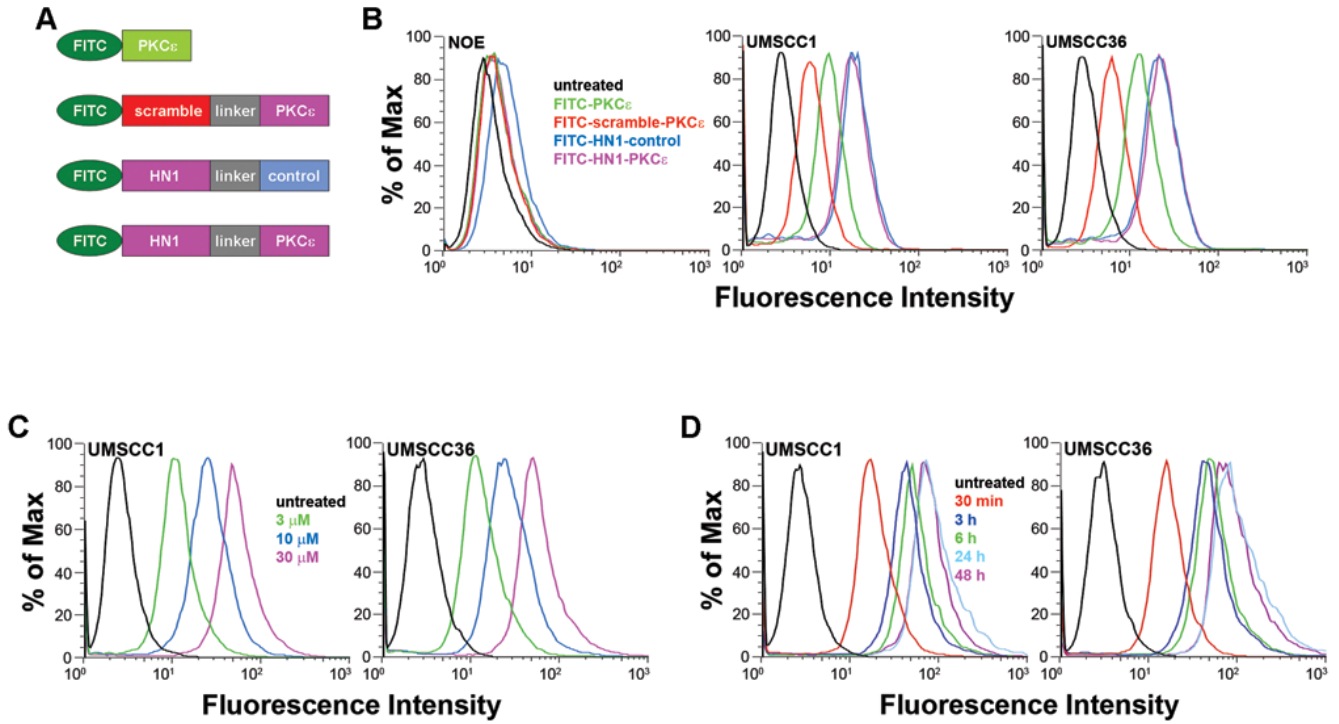


Figure 1.

HN1-PKCε selectively penetrates HNSCC cells *in vitro*. A. Schematic diagram of FITC-labeled peptides. HN1 module: cancer cell homing peptide. Scrambled module: nonfunctional scrambled HN1 module. Linker module: linker peptide. PKCε module: PKCε inhibitory peptide: Control module: non-functional scrambled PKCε module. Peptides were end-capped (5'-acetylated and 3'-amidated) to enhance stability. B. HN1-PKCε preferentially internalizes into HNSCC *in vitro*. Normal oral epithelial cells (NOE), and HNSCC cells, UMSSCC1 and UMSSCC36, were untreated or incubated with FITC-labeled peptides (3μM) for 48 hours. Cells were harvested and analyzed by FACS. B. Dose-dependent internalization of HN1-PKCε into HNSCC cells. UMSSCC1 and UMSSCC36 cells were untreated or incubated with 3, 10, or 30 μM HN1-PKCε for 48 hours. Cells were harvested and analyzed by FACS. C. Time-dependent internalization of HN1-PKCε into HNSCC cells. UMSSCC1 and UMSSCC36 cells were untreated or incubated with 30 μM HN1-PKCε for 30 minutes, 3, 6, 24, or 48 hours. Cells were harvested and analyzed by FACS. These histograms are representative of several independent experiments.

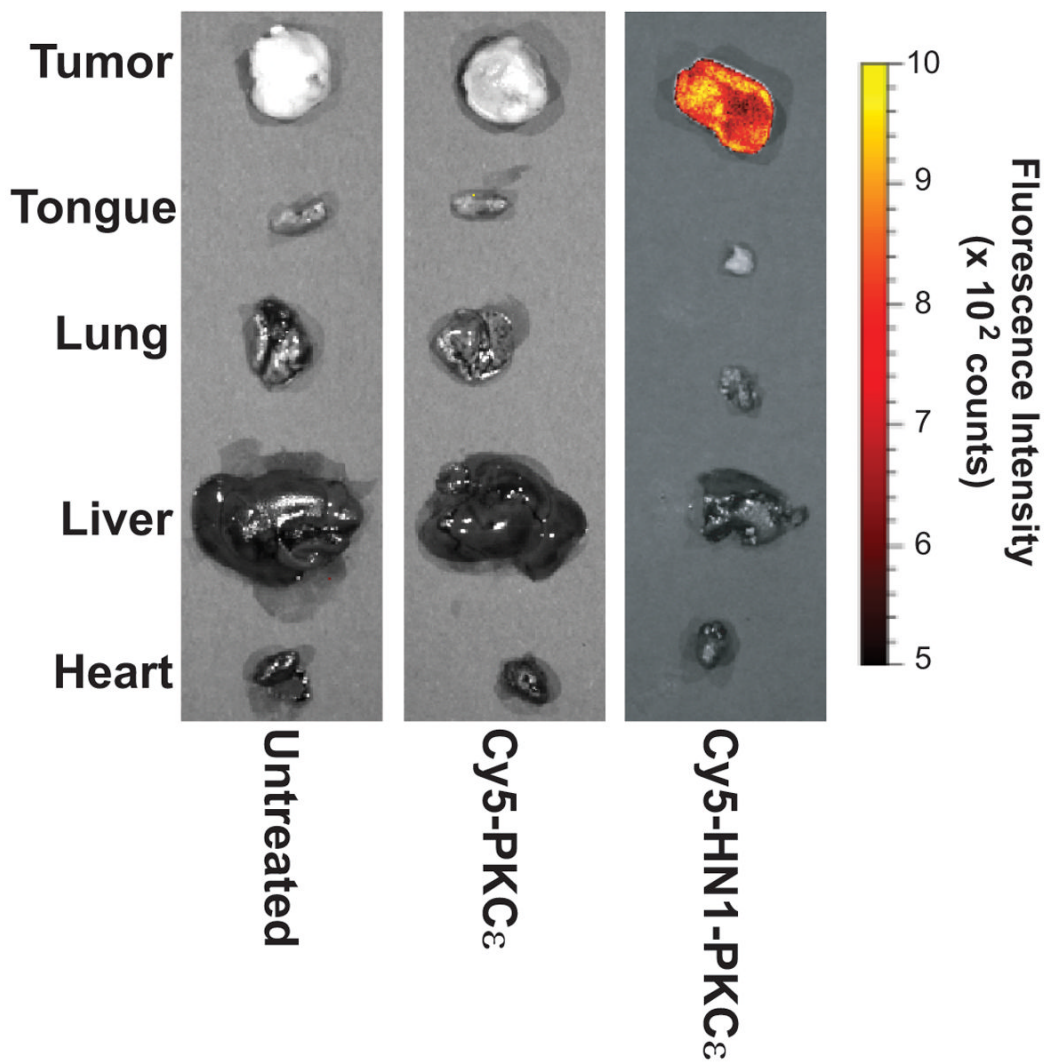


Figure 2. HN1-PKC ϵ selectively homes to HNSCC xenografts *in vivo*. Nude mice with established UMSSC1 tumors in the flank were untreated or treated with Cy5-labeled HN1-control or HN1-PKC ϵ (IP injection, 10 mg/kg). After 24 hours, mice were euthanized and tumors and various organs were resected for fluorescence intensity analysis using the Xenogen IVIS Spectrum Imaging System.

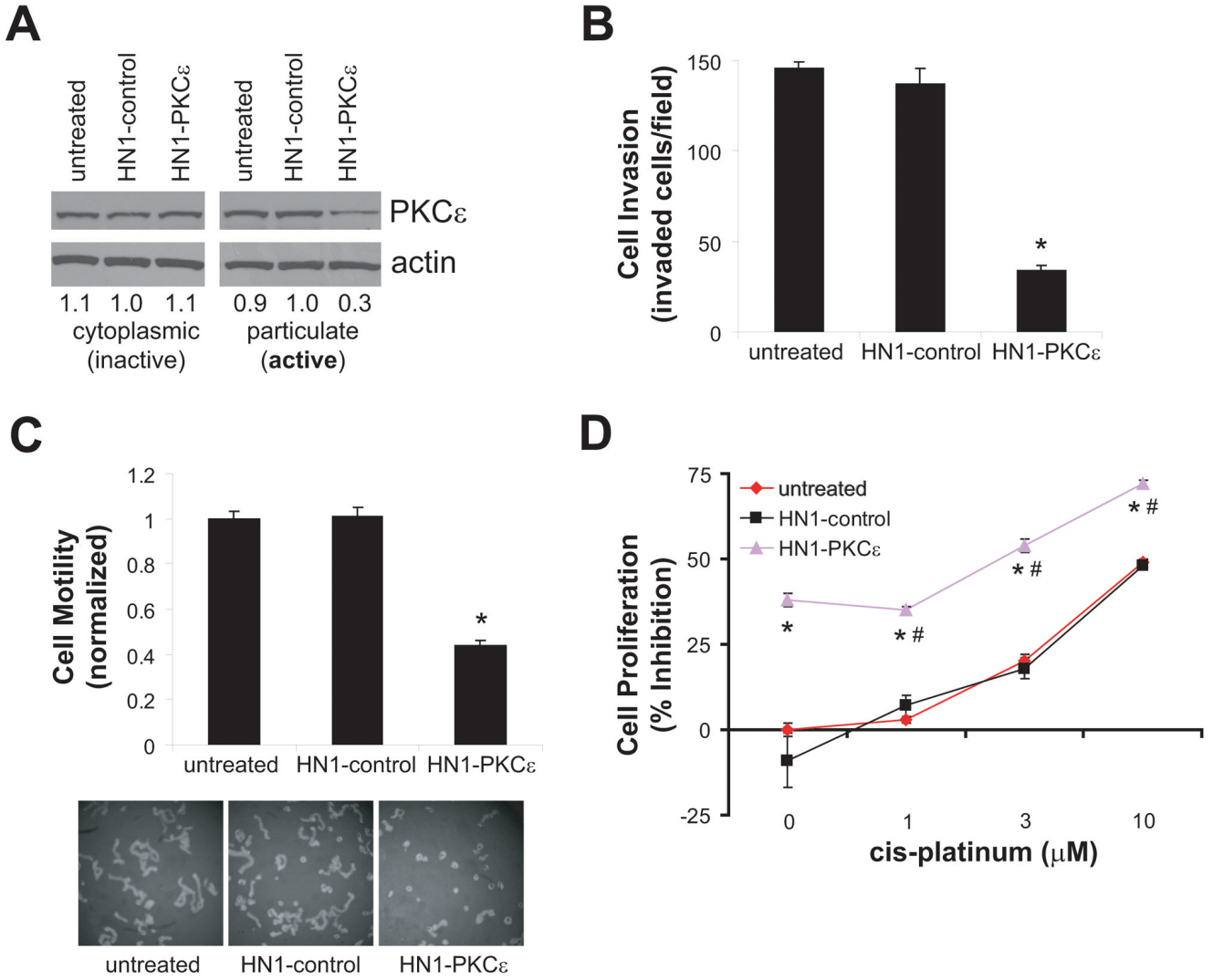


Figure 3. HN1-PKC ϵ blocks active PKC ϵ translocation and inhibits cell invasion, motility, and proliferation. **A.** HN1-PKC ϵ disrupts localization of active PKC ϵ in HNSCC cells. Inactive and active PKC ϵ levels were detected by western blot analysis with an anti-PKC ϵ antibody. Bands were quantified by densitometry and data is presented as fraction of PKC ϵ levels relative to the HN1-control-treated cells. **B.** HN1-PKC ϵ inhibits cell invasion. Cell invasion was assessed using the Modified Boyden chamber invasion assay with Matrigel basement membrane. Invasive cells were counted and presented as invaded cells per field. * p-value < 0.001, n=12. **C.** HN1-PKC ϵ inhibits cell motility. Cell motility was assessed using the 2-dimensional random cell motility assay. Cells were fixed and areas of clearing in the microbead field corresponding to phagokinetic cell tracks were quantified using NIH ScionImager. * p-value < 0.001, n=5. **D.** HN1-PKC ϵ inhibits cell proliferation. Cell proliferation was determined using the MTT assay. * p-value < 0.006, n=4; HN1-PKC ϵ compared to HN1-control or cis-platinum. # p-value < 0.001, n=4; monotherapy HN1-PKC ϵ compared to combination regimen of HN1-PKC ϵ and cis-platinum.

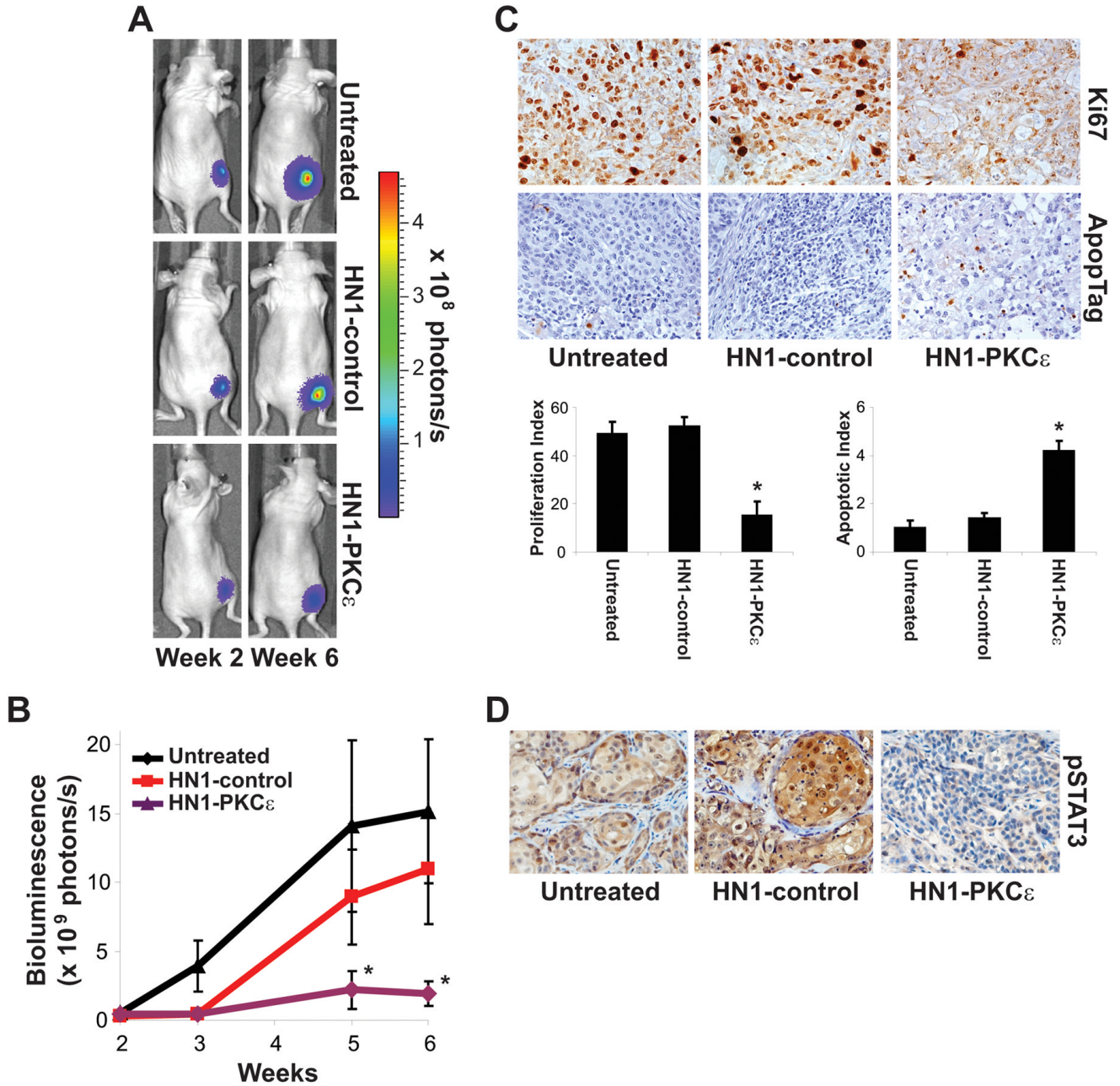


Figure 4. HN1-PKC ϵ retards tumor growth in a pre-clinical model of HNSCC. **A.** Bioluminescence images from a representative mouse in the untreated arm, HN1-control treatment arm, and HN1-PKC ϵ treatment arm. **B.** Bioluminescence. Tumor bioluminescence activity was measured using the Xenogen IVIS Spectrum Imaging System. * p-value < 0.02. **C.** Tumor proliferation and apoptotic index. Tumor sections were stained for proliferating cells using an anti-Ki67 antibody (DAKO, Denmark) and apoptotic cells using the ApopTag kit (Intergen Company, Purchase, NY). Proliferation and apoptotic index was determined by counting the number of Ki67- and TUNEL-positive cells per 500 total cells in five separate random fields at high power (400X). * p-value < 0.001. **D.** Tumor pSTAT (S727) levels. Tumor section were

stained for S727-phosphorylated Stat3 using an anti-phospho-S727-Stat3 antibody (Cell Signaling, Beverly, MA). These are representative sections for each treatment arm.